The β decay in this system is not easily understood and gives evidence of an unfamiliar selection rule. Our experiment suggests that the $L=1$ components of first-forbidden β decay to the five levels in question are retarded or absent. This in turn may explain the absence of β decay to the $\frac{7}{2}+$ ground state, the possible absence of decay to the 410-kev spin $\frac{3}{2}+$ state, and the $L=0$ character of the β branches to the other three states. These $L=0$ assignments are obtained indirectly and we cannot place very much confidence in them. A different experiment to check this point would be very desirable. Among such experiments are (a) direct measurement of the β-particle anisotropy, and (b) measurement of the γ-ray anisotropies at a temperature low enough to produce saturation of the alignment.

APPENDIX

After this paper had been written we received a communication from G. T. Ewan *et al.*[28] They had made spin and parity assignments for the excited states of Pm^{147} identical to ours, except that they had not eliminated the $\frac{3}{2}+$ possibility for the 686-kev state. Their multipolarity assignments for the mixed γ rays were in good agreement with ours. Such agreement between independent measurements is very encouraging, and we conclude that these experimental aspects of the decay of Nd^{147} are well understood. A theoretical explanation of the β decay would be very interesting.

[28] G. T. Ewan, R. L. Graham, and J. S. Geiger, Bull. Am. Phys. Soc. **6**, 238 (1961).

PHYSICAL REVIEW VOLUME 123, NUMBER 5 SEPTEMBER 1, 1961

Proton Interactions with Cu^{63} and Cu^{65}†

J. BENVENISTE, R. BOOTH, AND A. MITCHELL
Lawrence Radiation Laboratory, University of California, Livermore, California

(Received April 20, 1961)

Elastic scattering of protons from Cu^{63} and Cu^{65} has been observed for several energies in the range 7 to 12 Mev. When plotted as the ratio-to-Rutherford, the isotopic differential cross sections exhibit a shift which is two to three times larger than would be expected if the nuclear radius were governed by the $A^{\frac{1}{3}}$ law.

Inelastic scattering and (p,α) cross sections were measured to contribute to our knowledge of the reaction cross sections and to an unambiguous optical-model analysis.

I. INTRODUCTION

THE optical model has been remarkably successful[1–10] in describing, quantitatively, cross sections for the interaction of protons with a wide range of nuclei over a large spectrum of energies. This success has prompted workers in the field to perform experiments designed to test more severely some of the broad conclusions of the model. As a result, there were discovered large differences[11–16] in the differential cross sections of neighboring nuclei which were puzzling in the light of optical-model predictions for changes much more gradual with A. These differences were most clearly revealed at back angles where the elastic-scattering cross sections for even-Z nuclei were found to be generally larger than for odd-Z nuclei. It was also found that whereas the angular distributions for odd nuclei could be well reproduced with optical-model calculations, those for neighboring even-Z nuclei gave considerable trouble if they yielded to analysis at all.

The interesting suggestion was put forth that these differences could be understood in terms of a compound elastic contribution which was smaller in the case of odd-Z nuclei because of competition from the greater number of exit channels. This is because the (p,n) threshold is generally considerably lower in odd-Z

† This work was performed under the auspices of the U. S. Atomic Energy Commission.

[1] R. D. Woods and D. S. Saxon, Phys. Rev. **95**, 577 (1954).
[2] M. A. Melkanoff, S. A. Moszkowski, J. S. Nodvik, and D. S. Saxon, Phys. Rev. **101**, 507 (1956).
[3] F. Bjorklund, S. Fernbach, and N. Sherman, Phys. Rev. **101**, 1832 (1956).
[4] M. A. Melkanoff, J. S. Nodvik, D. S. Saxon, and R. D. Woods, Phys. Rev. **106**, 793 (1957).
[5] A. E. Glassgold, W. B. Cheston, M. L. Stein, S. B. Schuldt, and G. W. Erickson, Phys. Rev. **106**, 1207 (1957).
[6] A. E. Glassgold and P. J. Kellogg, Phys. Rev. **107**, 1372 (1957).
[7] F. Bjorklund and S. Fernbach, *Proceedings of Second United Nations International Conference on the Peaceful Uses of Atomic Energy, Geneva, 1958* (United Nations, Geneva, 1958), Vol. 14, p. 24.
[8] R. Beurtey, Guillou, and J. Raynal, J. phys. radium **21**, 402 (1960).
[9] V. Meyer and N. M. Hintz, Phys. Rev. Letters **5**, 207 (1960).
[10] R. D. Albert and L. F. Hansen, Phys. Rev. Letters **6**, 13 (1961).
[11] D. A. Bromley and N. S. Wall, Phys. Rev. **107**, 1560 (1956).
[12] A. P. Klyucharev, L. I. Bolotin, and V. A. Lutsik, J. Exptl. Theoret. Phys. (U.S.S.R.) **30**, 573 (1956) [translation: Soviet Phys.—JETP **3**, 463 (1956)].
[13] W. F. Waldorf and N. S. Wall, Phys. Rev. **107**, 1602 (1957).
[14] M. Kondo, T. Yamazaki, A. Toi, R. Nakasima, and S. Yamabe, J. Phys. Soc. Japan **13**, 231 (1958).
[15] M. K. Brussel and J. H. Williams, Phys. Rev. **114**, 525 (1959).
[16] C. A. Prescott and W. P. Alford, Phys. Rev. **115**, 389 (1959).

nuclei, and inelastic scattering is expected to be more probable because of the greater density of final states.

Data from isotopes are not expected to be so strongly subject to these considerations. In spite of this, recent observations[17–24] from isotopes reveal differences pertinent to the development of the optical model. It was to contribute to these observations that our study of the copper isotopes was undertaken.

II. EXPERIMENTAL GEOMETRY

Figure 1 is a schematic diagram of the beam geometry. After emerging from the cyclotron, the beam is focused at the quadrupole lens Q_1. At M, it is deflected through an angle of about 25° into a second quadrupole lens Q_2. The magnet M_2 provides a small amount of steering or translation of the beam into S_1, an adjustable four-jaw collimator where preliminary collimation takes place. Final collimation of the beam to a diameter of $\frac{1}{8}$ in. occurs in the set of collimators and antiscattering diaphragms S_2 just ahead of the scattering chamber.

The scattering chamber is 40 in. in diameter. At its center is an eight-position target holder which is remote controllable. On a rotatable table within the chamber are mounted radial tracks on which detectors may be quickly and accurately mounted. Table motion is remote controlled and the table position readout, at a digital voltmeter in the control room, is precise to ±0.10°.

After traversing the scattering chamber, the unscattered beam is collected in the Faraday cup F. The diameter of the Faraday cup is 3 in. Its size and position were selected so that the solid angle it subtends at the target is sufficiently large that none of the beam multiply scattered in the target is lost. Suppression of secondary electrons produced in the Faraday cup by the incident beam is accomplished by means of a negatively charged grid placed just ahead of the cup. Bias curves, run by observing the number of particles scattered into a detector per unit charge collected by the Faraday cup, indicate that a plateau is achieved for bias voltages larger than −20 v. Subsequent experiments were conducted with a bias voltage of −50 v. The charge collected in the Faraday cup was measured with a precision of 1%.

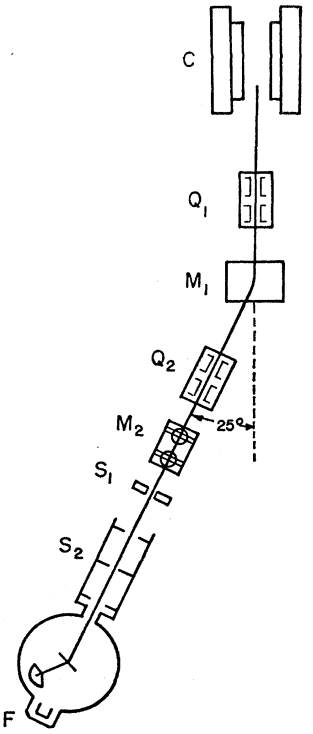

FIG. 1. Schematic diagram of cyclotron beam geometry.

III. ENERGY MEASUREMENT AND CONTROL

Beside the entrance hole to S_2 and separated from it by 0.030 in. is another hole. The beam entering this hole is scattered 90° through a variable absorber into a double proportional counter. An anticoincidence arrangement permits us to make a range measurement of the incident beam. We feel that we can measure the beam energy with a precision about equal to that of the range-energy data, say ±1%.

Back of the proportional counter is a NaI(Tl) crystal and photomultiplier tube. After the range has been measured, only enough absorber is left in to allow about 1 Mev to be deposited in the crystal. Pulses from the photomultiplier tube are fed into our "continuous energy monitor"—a device which measures the average height of input pulses and yields a continuously visible meter reading. Sensitivity checks show that in the course of our runs it was possible to keep the incident energy constant to ±0.15%.

IV. DETECTOR

The detector consists of a NaI(Tl) crystal and photomultiplier tube preceded by a gas proportional counter with offset center wire. Signals from the gas counter (proportional to dE/dX) and from the NaI(Tl) crystal (proportional to the energy E) are fed into the two sides of a pulse multiplier network. Then since dE/dX is approximately proportional to MZ^2/E, the output

[17] R. Beurtey, P. Catillon, R. Chaminade, H. Faraggi, A. Papineau, and J. Thirion, Nuclear Phys. **13**, 397 (1959).
[18] R. A. Vanetsian, A. P. Klyucharev, and E. D. Fedchenko, Atomnaya Energ. **6**, 661 (1959).
[19] S. Kobayashi, K. Matsuda, Y. Nagahara, Y. Oda, and N. Yamamuro, J. Phys. Soc. Japan **16**, 1151 (1960).
[20] N. Ya Rutkevich, V. Ya Golovnya, A. K. Val'ter, and A. P. Klyucharev, Doklady Akad. Nauk S. S. S. R. **130**, 1008 (1960) [translation: Soviet Phys.—Doklady **5**, 118 (1960)].
[21] A. P. Klyucharev and N. Ya Rutkevich, J. Exptl. Theoret. Phys. (U.S.S.R.) **38**, 285 (1960) [translation: Soviet Phys.—JETP **11**, 207 (1960)].
[22] A. K. Val'ter, I. I. Zalyubrovskii, A. P. Klyucharev, M. V. Pasechnik, N. N. Pucherov, and V. I. Chirko, Zhur. Eksptl. i Teoret. Fiz. **38**, 1419 (1960).
[23] P. C. Gugelot, *Proceedings of the International Conference on Nuclear Structure, Kingston*, edited by D. A. Bromley and E. W. Vogt (University of Toronto Press, Toronto, 1960), p. 715.
[24] C. B. Fulmer (private communication, to be published).

from this network will identify the detected particle as a proton, deuteron, α particle, etc. Electronic corrections are made to the signals to take account of the facts that dE/dX is not strictly proportional to $1/E$ and that not all the particle energy is deposited in the crystal. For diagnostic purposes, an oscilloscope display was devised showing the output of the multiplier circuit on the vertical sweep versus the particle energy on the horizontal sweep. With this display it was possible to quickly and accurately adjust the circuit parameters for optimum particle discrimination.

V. TARGETS

Self-supporting foils of the two isotopes were prepared at this laboratory by a vacuum deposition technique. The average thickness of each foil was determined by first measuring the area with a traveling microscope, then carefully weighing the foil on a microbalance. With Verni-Ray,[25] an instrument designed for measuring the uniformity of thin foils, there were found no variations larger than 4% of the average thickness in the region intercepted by the beam. The mean variation was found to be considerably smaller than this so that no correction from the average thickness measurement was necessary.

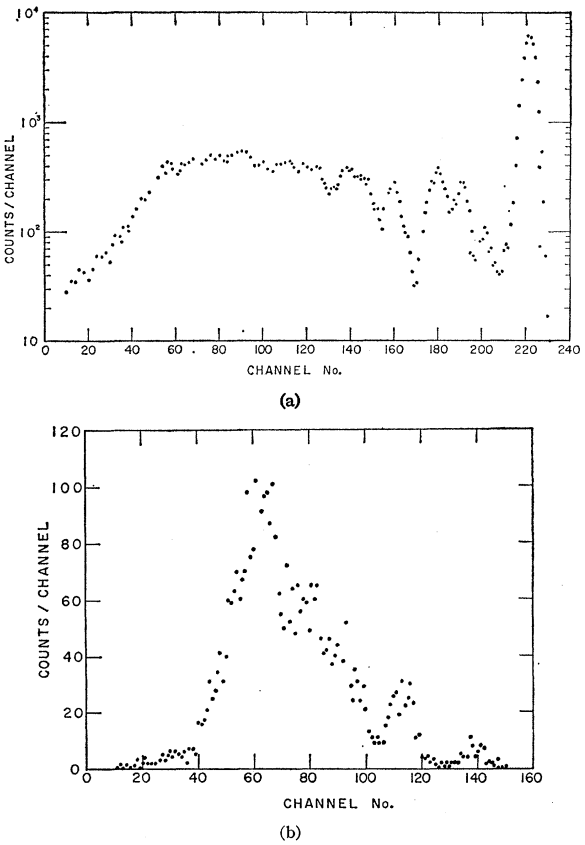

FIG. 2. Typical spectra of scattered particles from proton reactions on Cu^{63}; E_p=8.80 Mev. (a) For $Cu^{63}(p,p')$, where θ=120°. (b) For $Cu^{63}(p,\alpha)$, where θ=90.8°.

[25] J. Benveniste, R. Booth, A. Mitchell, C. D. Schrader, and J. Zenger, University of California Radiation Laboratory Report UCRL-6049, 1960 (to be published).

TABLE I. Proton reaction cross sections, in mb.

E_p(Mev)	Cu^{63} $\sigma(p,p')$	Cu^{63} $\sigma(p,\alpha)$	Cu^{63} $\sigma(p,q)$	Cu^{65} $\sigma(p,p')$	Cu^{65} $\sigma(p,\alpha)$	Cu^{65} $\sigma(p,q)$
5.19			173±20			49±10
6.20	215±25	35±3	250±25	56±32	37±10	93±30
7.34			242±15			68±10
8.80	303±20	61±4	364±20[a]	112±15	26±3	138±15[a]
9.85[a]			365±18			155±10
10.20	340±20	66±2	406±20	150±20	22±1	172±20
11.03	394±20	70±2	464±20	157±10	34±3	191±11
12.3			486±30			219±15

[a] A value of $\sigma(p,q)$ =266 mb for 7.5-Mev protons on normal Cu has been reported by B. W. Shore, N. S. Wall, and J. W. Irvine, Jr., Bull. Am. Phys. Soc. 5, 424 (1960).

Isotopic purity of the target material was checked twice, first in its original form by Oak Ridge National Laboratory, the supplier, then again after fabrication by M. C. Michel of our Berkeley laboratory. The results, appearing below, are in excellent agreement:

		ORNL	Berkeley
"63"	Cu^{63}	99.40%	99.55%
	Cu^{65}	0.60%	0.45%
"65"	Cu^{65}	98.16%	97.8%
	Cu^{63}	1.84%	2.2%

VI. EXPERIMENTAL PROCEDURE

These experiments were performed with the aid of "Scatterbrain," a control system which conducts most of the necessary routine operations. Briefly, Scatterbrain will select a scattering angle according to initial instructions, move the detector to the selected angle, reset the scalers, clock, beam-current integrator, and multichannel analyzer, start the accumulation of data, and continue the run until a preset charge setting has been reached. All the data pertinent to the run may then be read out on printed tape and/or punched paper tape. Upon completion of the cycle, a new angle is automatically selected and the cycle is repeated. Successive observations were customarily made in 30° steps. The first sweep was begun at 30°, the second sweep, at 20°. After a third sweep, begun at 40°, data were available every 10° in the interval from 20° to 170°. Further sweeps were made when finer observations were desired. That the entire angular interval was studied in at least three sweeps meant that any instrumental drifts would have been readily revealed. The two copper isotopes were mounted in adjacent slots of the target changer and observations on the two were made successively at each angle setting.

VII. RESULTS AND CONCLUSIONS

With our particle identifier it was possible to measure (p,p') and (p,α) cross sections separately just by selecting the proper gate for the multichannel analyzer. Sample spectra appear in Fig. 2. These observations

TABLE II. Elastic scattering of protons by Cu^{63} and Cu^{65}.

$\theta_{c.m.}$ (deg)	$\sigma(\theta)$ (mb/sr) Cu^{63}	±%	Cu^{65}	±%
	E_p=12.29 Mev			
19.2	6147	1.7	6086	1.7
29.6	1502	1.4	1523	1.4
40.0	255.7	1.4	484.0	1.4
50.8	137.0	1.7	124.0	1.7
61.4	32.3	1.7	27.3	1.7
65.3	22.5	1.7	22.7	1.7
71.0	18.7	2.4	23.5	2.4
75.4	21.0	2.4	27.3	2.4
80.4	24.1	2.4	29.4	2.4
86.5	27.4	2.5	28.4	2.5
90.0	25.8	2.0	27.4	2.0
95.4	23.4	2.5	22.8	2.5
101.1	18.4	2.4	16.6	2.4
105.7	14.4	2.4	10.5	2.4
110.8	9.73	2.4	6.23	2.4
115.6	5.52	3.2	3.32	3.2
120.3	3.04	3.2	2.19	3.2
125.8	1.57	3.2	1.57	3.2
130.8	1.34	4.2	2.00	4.2
135.9	2.29	3.2	2.96	3.2
140.5	3.67	3.2	5.08	3.2
145.6	6.32	3.2	6.40	3.2
152.7	8.41	2.4	8.09	2.4
160.5	11.4	2.4	9.98	2.4
165.1	13.1	2.4	10.9	2.4
	E_p=11.03 Mev			
20.8	7113	1.7	7384	1.7
30.3	1823	1.7	1917	1.7
40.7	629.3	1.7	602.0	1.7
51.3	181.0	1.7	150.4	1.7
56.3	86.9	1.7	73.5	2.4
61.3	46.0	1.4	38.5	1.4
66.5	25.9	3.2	27.1	3.2
71.6	23.5	2.4	27.6	1.7
76.5	24.6	3.2	32.5	3.2
81.7	27.6	2.4	34.3	2.5
91.8	27.6	1.7	32.9	1.7
101.9	23.2	2.5	22.4	2.5
111.9	13.7	2.5	11.2	3.2
121.8	5.7	2.5	3.78	2.5
126.2	3.4	3.2	2.5	3.2
131.9	2.2	3.2	2.2	3.2
136.8	2.5	3.2	3.0	3.2
142.0	4.0	3.2	4.4	3.2
146.7	6.1	3.2	6.6	3.2
151.8	9.1	1.7	9.3	1.7
161.9	13.3	2.4	14.2	2.4
166.8	15.8	3.2	16.4	3.2
	E_p=10.20 Mev			
20.1			10213	1.7
25.3	3720	1.7	4013	1.7
30.3	2050	1.7	2252	1.7
35.8	1173	1.7	1183	1.7
40.4	758	1.7	734.1	1.7
50.4	239.5	1.7	207.5	1.7
56.0	114.6	1.7	95.8	1.7
61.1	60.3	1.7	53.0	1.7
66.4	35.1	1.7	32.9	1.7
71.5	27.8	1.7	31.7	1.7
76.5	28.4	1.7	34.2	1.7
80.8	30.8	1.7	37.7	1.7
86.7	34.7	1.7	39.4	1.7
91.8	34.8	1.7	38.2	1.7
96.8	33.8	1.7	34.6	1.7
101.8	29.7	1.7	27.3	1.7
106.8	25.1	1.7	20.5	1.7
110.9	20.4	1.7	16.9	1.7
116.8	13.7	1.7	10.7	1.7
121.9	9.23	1.7	6.75	1.7
126.7	5.80	1.7	4.00	1.7
132.0	4.36	2.4	2.82	2.4
136.8	3.77	2.4	3.07	2.4
140.7	4.10	2.4	4.03	2.4
146.8	6.26	1.7	6.60	1.7
151.7	8.22	1.7	9.21	1.7
156.7	11.46	1.7	12.11	1.7
161.7	13.68	1.7	15.03	1.7
169.4	16.72	1.7	18.0	1.7
	E_p=8.80 Mev			
20.4	13134	1.7		
30.6	2963	1.7	3047	1.7
40.8	1017	1.7	1016	1.7
51.4	324.1	1.7	305.5	1.7
60.5	107.1	1.7		
66.3	62.2	1.7	63.1	1.7
71.8	42.9	1.7	44.2	1.7
76.7	38.1	1.7	38.7	1.7
81.8	40.6	1.7	47.1	1.7
86.8	43.5	1.7	49.5	1.7
92.0	45.9	1.7	50.6	1.7
97.2	46.8	1.7	48.4	1.7
102.1	40.0	1.7	42.9	1.7
111.9	34.4	1.7	29.7	1.7
122.2	21.6	1.7	16.7	1.7
132.8	11.7	2.2	8.41	2.2
141.6	7.77	2.4	5.96	2.4
150.7	7.44	2.4	6.11	2.4
162.2	10.13	2.2	11.65	2.2
168.2	12.2	2.2	13.54	2.2
	E_p=7.34 Mev			
20.6	22045	2.4	22240	2.4
30.6	4510	2.4	4534	2.4
35.8	2482	2.4	2434	2.4
40.9	1510	2.4	1494	2.4
51.1	579.2	2.4	554	2.4
71.4	97.6	2.4	92.7	2.4
76.5	73.5	2.4	73.2	2.4
81.5	63.5	2.4	66.6	2.4
86.1	62.1	2.4	67.8	2.4
91.1	59.9	2.4	65.2	2.4
111.6	50.5	2.4	52.7	2.4
120.1	41.9	3.2	41.4	3.2
131.3	29.8	3.2	25.3	3.2
141.2	19.8	3.2	16.3	3.2
151.2	12.6	4.2	10.2	4.2
161.5	10.2	4.2	8.4	4.2

were customarily made at 30, 60, 90, 120, and 150 deg. In each case contributions due to the impurities H, C, and O were identified and subtracted prior to calculating a differential cross section. A smooth curve drawn through these points was integrated over all angles to yield the required cross section. It was necessary to correct the inelastic-scattering observations for slit-scattering effects. This was done by measuring the energy distribution of protons scattered from a thin gold foil, assuming that at these energies there should be only elastic scattering, and hence attributing all observed low-energy events to slit scattering. Upon normalizing the elastic peaks of the Au and Cu distributions, the correction to the Cu spectrum was found. This correction amounted to 1.5 to 2.0% of the elastic peak. A major contribution to the uncertainty quoted for the (p,p') cross sections is due to the large slit-scattering correction at 30° and the resulting poor information on the shape of the curve in this region.

Our charged-particle cross sections appear in Table I. These, together with (p,n) cross sections,[26–28] yield lower limits for proton reaction cross sections, which will contribute to an unambiguous optical-model analysis.

The results of our elastic-scattering measurements appear in Table II. The quoted errors include contributions from statistics, beam-current integrator measurements, and geometrical factors. Corrections due to finite angular resolutions and multiple scattering were investigated. The former effect was found to be insignificant; the latter contributes less than $\frac{3}{4}$% in the worst case.

Although differences are apparent, the representation in which the differences appear most strikingly is that of Figs. 3–7, where the ratios of differential cross

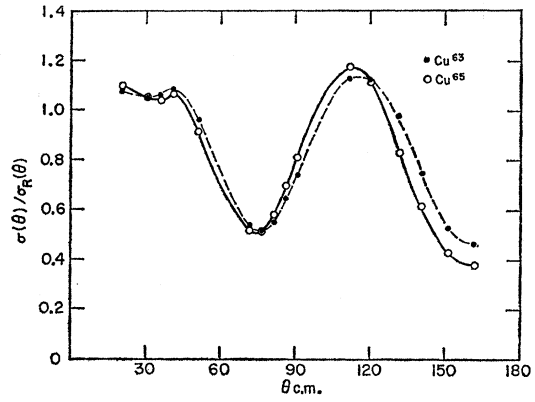

FIG. 3. Ratio of the measured differential cross section for elastic scattering to the Rutherford cross section; E_p=7.34 Mev.

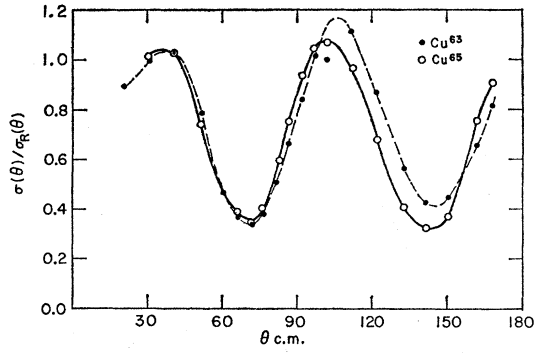

FIG. 4. Ratio of the measured differential cross section for elastic scattering to the Rutherford cross section; E_p=8.80 Mev.

[26] J. P. Blaser, F. Boehm, P. Marmier, and D. C. Peaslee, Helv. Phys. Acta **24**, 3 (1954).
[27] J. A. Howe, Phys. Rev. **109**, 2083 (1958).
[28] R. D. Albert and L. F. Hansen (private communication, to be published).

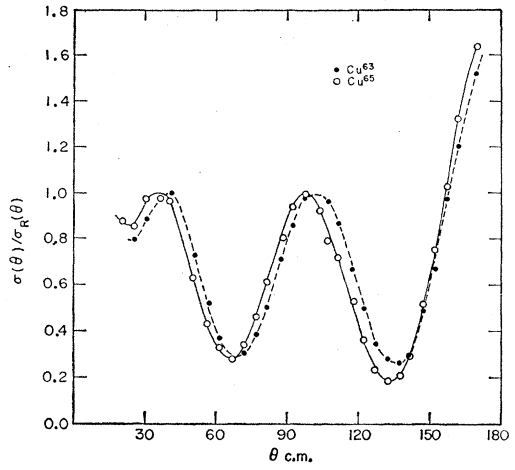

FIG. 5. Ratio of the measured differential cross section for elastic scattering to the Rutherford cross section; $E_p=10.20$ Mev.

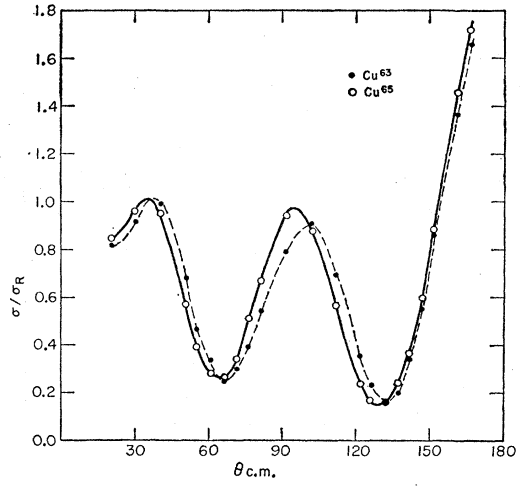

FIG. 6. Ratio of the measured differential cross section for elastic scattering to the Rutherford cross section; $E_p=11.03$ Mev.

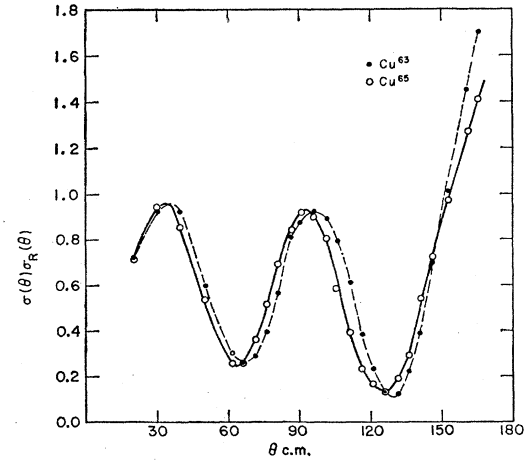

FIG. 7. Ratio of the measured differential cross section for elastic scattering to the Rutherford cross section; $E_p=12.29$ Mev.

sections to the Rutherford cross sections are displayed. This representation clearly shows a shift in the angular distribution, a shift in the same direction as that to be expected if Cu^{65} were larger than Cu^{63}; however, it is two to three times that expected if the nuclear radius were governed by the $A^{\frac{1}{3}}$ law. This can be seen by comparing Fig. 8, showing the shift given by the optical model of Bjorklund and Fernbach, with the experimental shift of Fig. 5 at the same energy.

It is conceivable that we need make only one optical-model parameter isotope-dependent to explain the observed effects. Small changes in either the nuclear radius or the real potential depth would give qualitative shifts of the type we seek, although the fact of their interrelation may make it difficult to decide between them. We would have thought that if the radius parameter were unusually isotope dependent, this would manifest itself most clearly in observations on α scattering. This is because optical-model analyses[29] have shown that for α particles, nuclei appear quite black (i.e., the radius parameter is critical but the potential can be almost anything). In fact, elastic-scattering data[30,31] do indicate departures from the $A^{\frac{1}{3}}$ law for isotopes and other neighboring nuclei. However, detailed optical-model calculations[8] have shown that a simple variation of the radius seems to be incapable of completely explaining the cross-section variations observed for protons and alpha particles on the Zn isotopes.

On the other hand, a number of papers[32–36] have appeared in which are made attempts to understand the source of the difference in the proton-nucleus and neutron-nucleus potentials. Some of these calculations may bear on our results.

Beginning with the Saxon potential, Sliv and Volchok have calculated the excitation energies for the first few levels of nuclei with doubly closed shells plus or minus one nucleon. The assumption is made that these are single-particle levels. Comparing the calculated energies with experimental data, they find that the potential parameters are the same for all nuclei lying on the stability curve. For nuclei off the stability curve, the change in the depth of the proton potential is given by

$$\Delta V=a(N-N_{\rm st})/A,$$

[29] G. Igo, Phys. Rev. Letters **1**, 72 (1958).
[30] D. D. Kerlee, J. S. Blair, and G. W. Farwell, Phys. Rev. **107**, 1343 (1957).
[31] R. Beurtey, P. Catillon, R. Chaminade, M. Crut, H. Farazzi, A. Papineau, J. Saudinos, and J. Thirion, J. phys. radium **21**, 399 (1960).
[32] A. A. Ross, H. Mark, and R. D. Lawson, Phys. Rev. **102**, 1613 (1956).
[33] A. A. Ross, R. D. Lawson, and H. Mark, Phys. Rev. **104**, 401 (1956).
[34] A. E. S. Green and P. C. Sood, Phys. Rev. **111**, 1147 (1958) —this paper contains a more complete bibliography.
[35] L. A. Sliv and B. A. Volchok, J. Exptl. Theoret. Phys. (U.S.S.R.) **36**, 539 (1959) [translation: Soviet Phys.—JETP **36**, 374 (1959)].
[36] G. R. Satchler, Phys. Rev. **109**, 429 (1958).

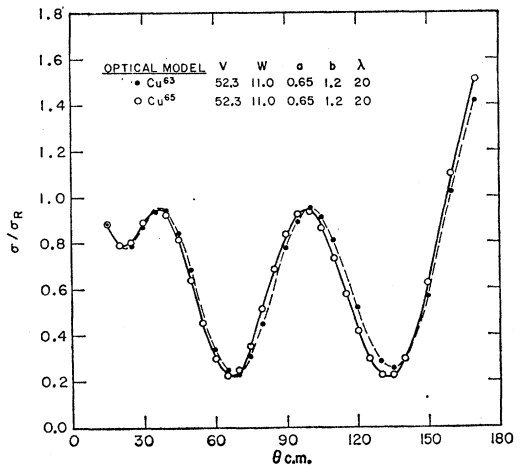

FIG. 8. Optical-model calculation showing shift in differential cross section expected if nuclear radius were governed by $A^{\frac{1}{3}}$ law; $E_p=10.20$ Mev.

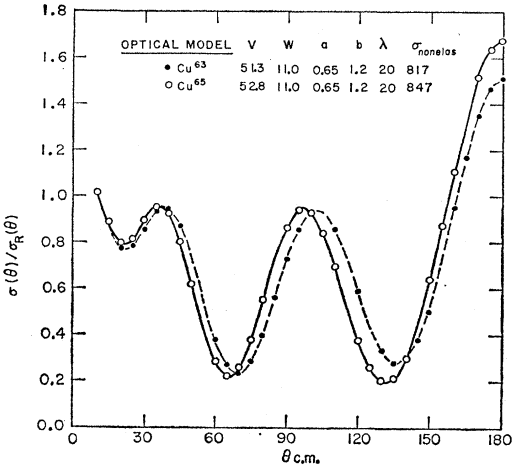

FIG. 9. Optical-model calculation which includes effect of proton potential anomaly; $E_p=10.20$ Mev. V is the real potential depth in Mev, W is the imaginary potential depth in Mev, a is the fall-off parameter in fermis, b is the width of the imaginary potential in fermis, and λ is the factor by which the Thomas term must be multiplied to yield the spin orbit potential. The nonelastic cross section is given in millibarns.

where $\Delta N=N-N_{st}$ is the departure of the neutron number from its value for nuclei on the stability curve, A is the mass number, and $a=80$ Mev. If these results may be applied to the copper isotopes, we should expect an increase in the real potential depth of Cu^{65} over Cu^{63} of 2.5 Mev.

Green and Sood calculate the proton potential by altering the neutron potential with the Coulomb perturbation and adjusting the proton potential anomaly to achieve the experimental binding energy for the last proton. They find for the potential anomaly

$$\Delta V=C_A(N-Z)/A,$$

where $C_A=57\pm4$. This yields for the two copper isotopes a potential difference of about 1.8 Mev. In Fig. 9 we show the effect of increasing the depth of the real well of Cu^{65} by 1.5 Mev. Comparison with Fig. 6 suggests that this correction comes quite close to explaining our present observations. Of course, the significance of this agreement awaits application to a broader range of observations.

ACKNOWLEDGMENTS

We gratefully acknowledge a number of stimulating and instructive discussions with our colleagues, R. D. Albert, F. Bjorklund, S. Fernbach, L. F. Hansen, H. Mark, and E. Schwarcz. Thanks are also extended to C. D. Schrader and J. Zenger for their participation in the early stages of this work. We are indebted to J. W. Frazer for reducing the original CuO and to William F. Brunner, Jr., for fabrication of the foils.